IECBM 2022
The 2nd International Electronic Conference on Biomolecules:
BIOMACROMOLECULES AND THE MODERN WORLD CHALLENGES
01–15 NOVEMBER 2022 | ONLINE

Modeling and simulation of magnetoliposomes formation by encapsulation of core-shell, magnetite-chitosan nanoparticles in liposomes enabled by a low-cost microfluidic system

Andres Mantilla-Orozco
MSc student(1)

Juan C. Cruz PhD(1)

Carolina Muñoz-Camargo PhD(1)

Andres Mantilla-Orozco(1), Cristian Rodríguez(1) ,Isabella Quiroz(1), Daniel Forero (1), María Camila Monsalve(1), Carlos E. Torres(1), Johann F. Osma PhD(2), Carolina Muñoz-Camargo. PhD(1) , Luis H. Reyes(3), Valentina Quezada(1), Juan C. Cruz. PhD (1)

(1) Department of Biomedical Engineering.
(2) Department of Chemical and Food Engineering
(3) Department of Electrical and Electronics Engineering

Universidad de los Andes Colombia | GINIB
biomolecules MDPI

Nanostructured materials applications

Nanobiotechnology

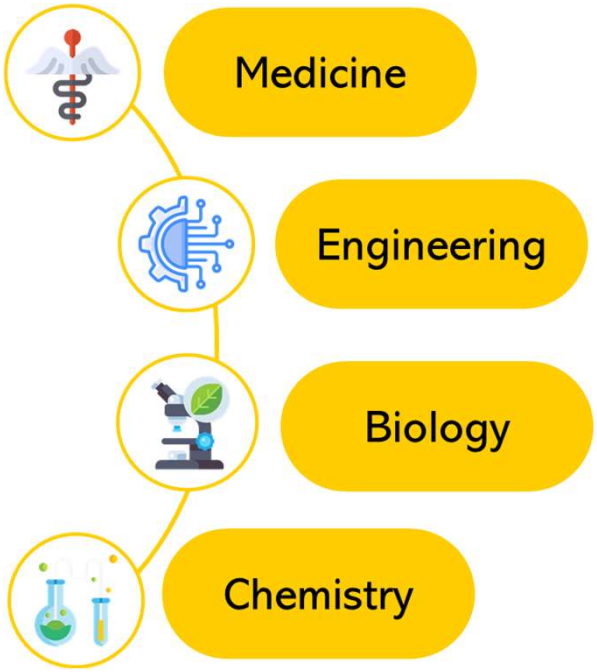

Michael Goldberg, Robert Langer, and Xinqiao Jia. Nanostructured materials for applications in drug delivery and tissue engineering. Journal of Biomaterials Science, Polymer Edition, 18(3):241–268, 2007.
Oliver Kayser, A Lemke, and Norma Hernandez-Trejo. The impact of nanobiotechnology on the development of new drug delivery systems. Current pharmaceutical biotechnology, 6(1):3–5, 2005.
Daniel G Anderson, Jason A Burdick, and Robert Langer. Smart biomaterials. Science, 305(5692):1923–1924, 2004.

Nanostructured materials applications

Nanobiotechnology

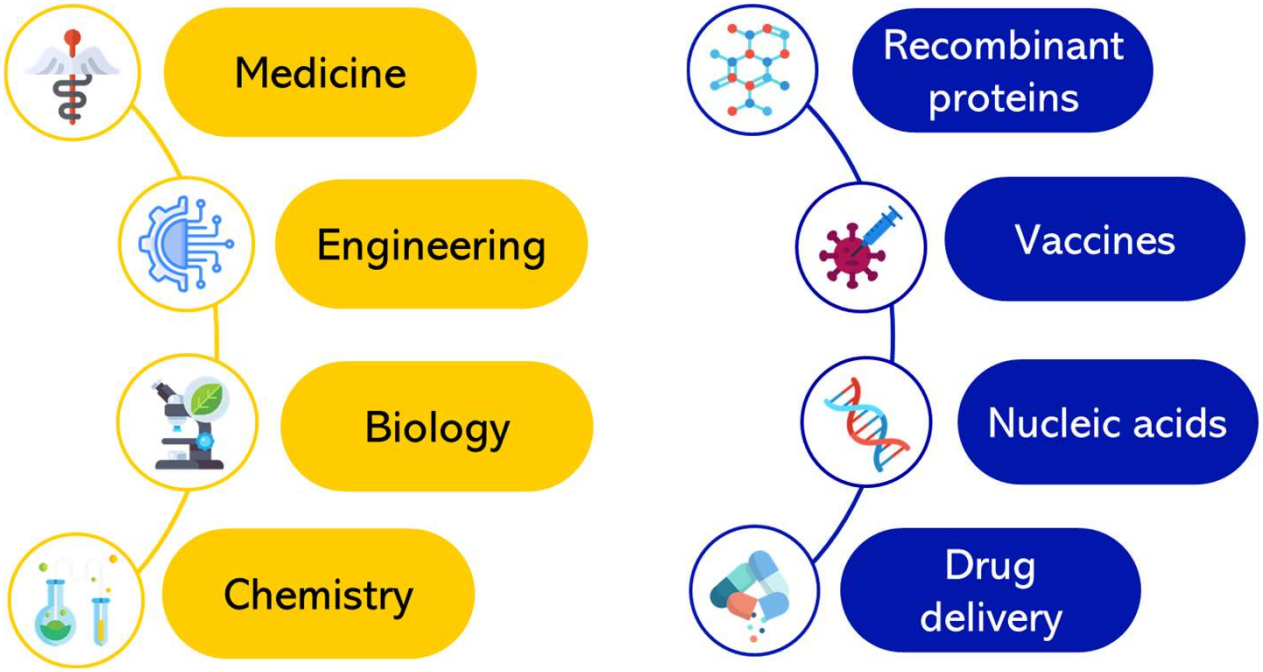

Andrei Kolmakov and Martin Moskovits. Chemical sensing and catalysis by one-dimensional metal-oxide nanostructures. Annu. Rev. Mater. Res., 34:151–180, 2004.
Lubhandwa S Biswaro, Mauricio G da Costa Sousa, Taia Rezende, Simoni C Dias, and Octavio L Franco. Antimicrobial peptides and nanotechnology, recent advances and challenges. Frontiers in microbiology, 9:855, 2018.

Nanostructured materials applications

Nanobiotechnology

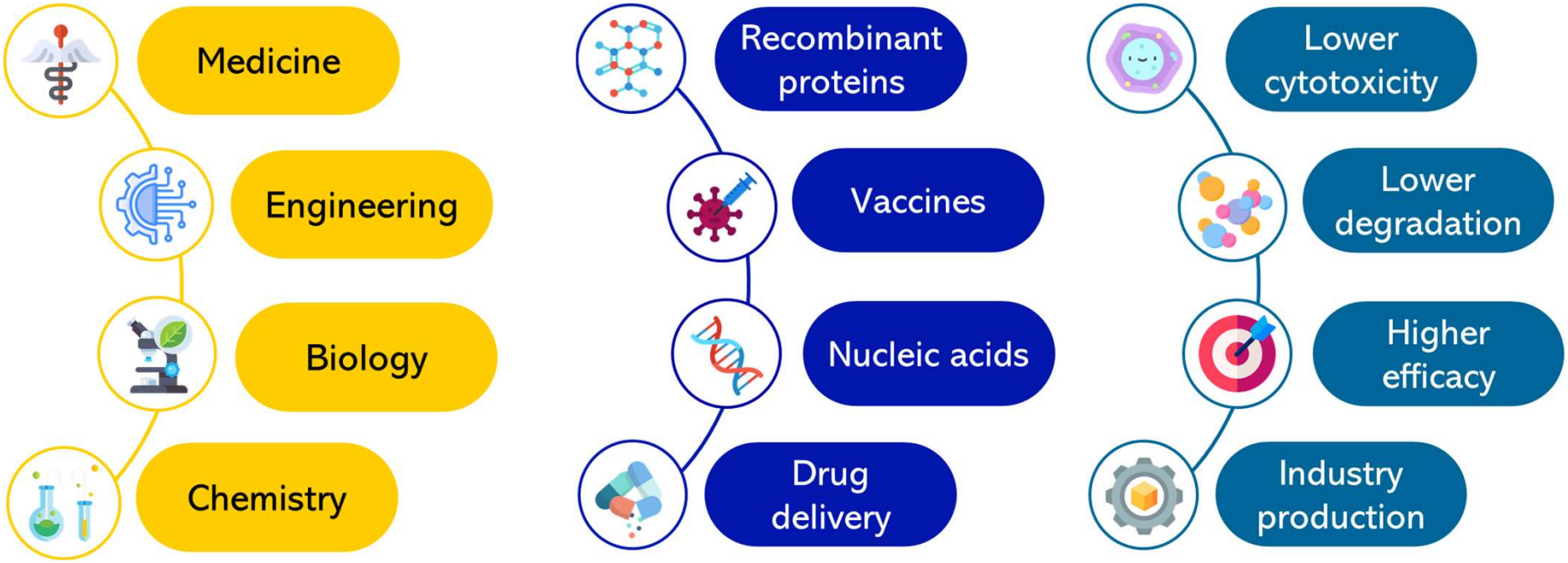

Afsaneh Lavasanifar, John Samuel, and Glen S Kwon. Poly (ethylene oxide)-block-poly (l-amino acid) micelles for drug delivery. Advanced drug delivery reviews, 54(2):169–190, 2002.
Yunus E Kurtoglu, Manoj K Mishra, Sujatha Kannan, and Rangaramanujam M Kannan. Drug release characteristics of pamam dendrimer–drug conjugates with different linkers. International journal of pharmaceutics, 384(1-2):189–194, 2010.
Yan Chen and Lihong Liu. Modern methods for delivery of drugs across the blood–brain barrier. Advanced drug delivery reviews, 64(7):640–665, 2012.

Nanotransporters advantages like drug delivery systems

Nanobiotechnology

Protection of peptides, vaccines and desired drugs against extracellular degradation

Selectivity of the target therapy

Improvement of the pharmacokinetic profile

Huilin Shao, Changwook Min, David Issadore, Monty Liong, Tae-Jong Yoon, Ralph Weissleder, and Hakho Lee. Magnetic nanoparticles and micronmr for diagnostic applications. Theranostics, 2(1):55, 2012.
Jin Xie, Gang Liu, Henry S Eden, Hua Ai, and Xiaoyuan Chen. Surface-engineered magnetic nanoparticle platforms for cancer imaging and therapy. Accounts of chemical research, 44(10):883–892, 2011.
Navin Kumar Verma, Kieran Crosbie-Staunton, Amro Satti, Shane Gallagher, Katie B Ryan, Timothy Doody, Colm McAtamney, Ronan MacLoughlin, Paul Galvin, Conor S Burke, et al. Magnetic coreshell nanoparticles for drug delivery by nebulization. Journal of Nanobiotechnology, 11(1):1–12, 2013.

Nanotransporters advantages like drug delivery systems

Nanobiotechnology

Protection of peptides, vaccines and desired drugs against extracellular degradation

Selectivity of the target therapy

Improvement of the pharmacokinetic profile

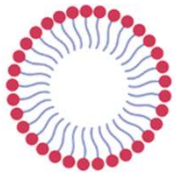

Micelles

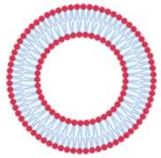

Liposomes

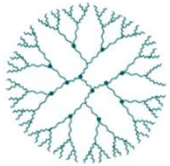

Dendrimers

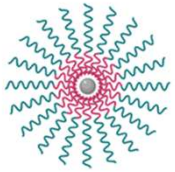

Polymeric nanoparticles

Huilin Shao, Changwook Min, David Issadore, Monty Liong, Tae-Jong Yoon, Ralph Weissleder, and Hakho Lee. Magnetic nanoparticles and micronmr for diagnostic applications. Theranostics, 2(1):55, 2012.
Jin Xie, Gang Liu, Henry S Eden, Hua Ai, and Xiaoyuan Chen. Surface-engineered magnetic nanoparticle platforms for cancer imaging and therapy. Accounts of chemical research, 44(10):883–892, 2011.

Nano bioconjugates compounds advantages

Liposomes/Nanopartices/AMP's

Liposomes

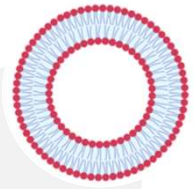

- Biocompatibility
- Biodegradability
- Encapsulate hydrophilic/hydrophobic compounds
- Similarity to cell's membranes
- Low cytotoxicity / High delivery rates

- Nanoparticles as drug delivery vehicles
- Iron oxide nanoparticles (Fe3O4)
- Advances in synthesis allows potential applications in diagnostic/therapeutic techniques.

Nanoparticles

Mingfeng Xie, Dijia Liu, and Yufeng Yang. Anti-cancer peptides: classification, mechanism of action, reconstruction and modification. Open Biology, 10(7):200004, 2020.
Su-Jin Kang, Do-Hee Kim, Tsogbadrakh Mishig-Ochir, and Bong- Jin Lee. Antimicrobial peptides: their physicochemical properties and therapeutic application. Archives of pharmacal research, 35(3):409– 413, 2012.
Fatma Gizem Avci, Berna Sariyar Akbulut, and Elif Ozkirimli. Membrane active peptides and

Nano bioconjugates synthesis technique

Microfluidics

- Manufacture devices to **outperforming** traditional analytical and sensing instruments employed in scientific research.
- **Development of several industries**: medical, cosmetics, pharma and food. Low cost devices
- Explored for the synthesis, manipulation, and separation of microscopic encapsulates.
- Explore in silico and in vitro species dynamics to understand **interaction between different phases in a system**

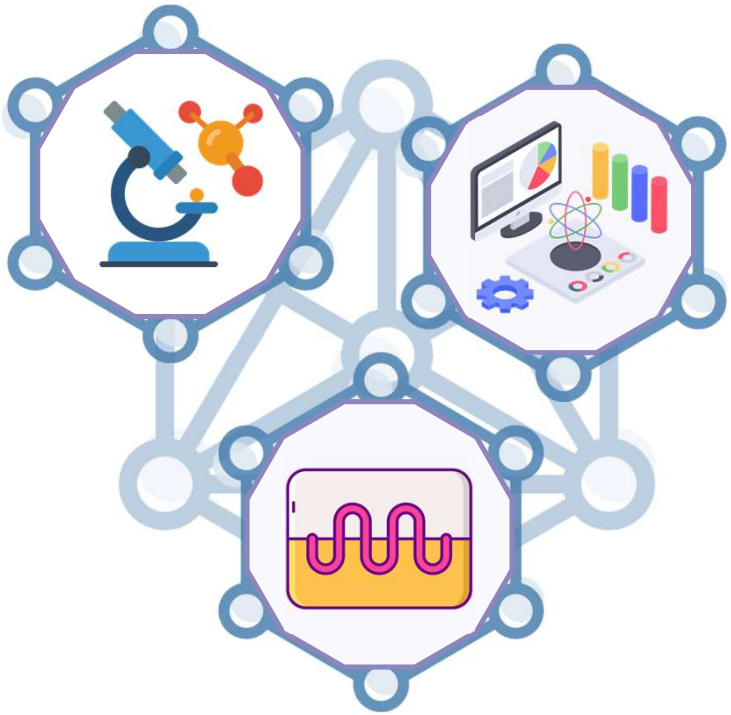

Mingfeng Xie, Dijia Liu, and Yufeng Yang. Anti-cancer peptides: classification, mechanism of action, reconstruction and modification. Open Biology, 10(7):200004, 2020.
Su-Jin Kang, Do-Hee Kim, Tsogbadrakh Mishig-Ochir, and Bong- Jin Lee. Antimicrobial peptides: their physicochemical properties and therapeutic application. Archives of pharmacal research, 35(3):409– 413, 2012.
Fatma Gizem Avci, Berna Sariyar Akbulut, and Elif Ozkirimli. Membrane active peptides and

Objectives

Implement multiphysics simulations to study *in silico* the encapsulation of core-shell, magnetite-chitosan nanoparticles in a microfluidic system by means of the COMSOL Multiphysics® software.

Euler-Euler (EE) Model

Liposome encapsulation of core-shell, magnetite-chitosan nanoparticles in a microfluidic system using a multiphase Euler-Euler computational model.

COMSOL Multiphysics Software

Euler-Euler (EE) model

Parameters

Material	Property	Value
H_2O	Density Dinamic Viscosity	$997\ [\mathrm{kg/m^3}]$ $8.9 \times 10^{-4}[\mathrm{Pa} * \mathrm{s}]$
CS-MNP´s	Density Diffusivity	$1100[\mathrm{kg/m^3}]$ $1.0 \times 10^{-9}[\mathrm{m^2/s}]$
Liposomes	Density Diffusivity	$1000[\mathrm{kg/m^3}]$ $1.51 \times 10^{-5}[\mathrm{m^2/s}]$

Inc., C. (2020). *COMSOL*. Retrieved from http://www.comsol.com/products/multiphysics/

Euler-Euler (EE) Model

Mass Balance

Continuity relations for continuous and dispersed phases

Continuous phase (liposomes)

$$\frac{\partial}{\partial t}(\rho_c \Phi_c) + \nabla \cdot (\rho_c \Phi_c u_c) = m_{dc}$$

Dispersed phase (CS-MNPs)

$$\frac{\partial}{\partial t}(\rho_d \Phi_d) + \nabla \cdot (\rho_d \Phi_d u_d) = -m_{dc}$$

Where

- $\Phi = volume\ fraction\ (dimensionless)$
- $\rho = density\left({}^{Kg}/_{m^3}\right)$
- $u = velocity\ (m/s)$
- $m_{dc} = mass\ transfer\ rate$

Inc., C. (2020). *COMSOL*. Retrieved from http://www.comsol.com/products/multiphysics/

Euler-Euler (EE) Model

Mass Balance

Relation between volume fractions. Continuous and dispersed phases considered incompressible

$$\Phi_c = 1 - \Phi_d$$

Continuous phase (liposomes)

$$\frac{\partial \Phi_c}{\partial t} + \nabla \cdot (\Phi_c u_c) = \frac{m_{dc}}{\rho_c}$$

Dispersed phase (CS-MNPs)

$$\frac{\partial \Phi_d}{\partial t} + \nabla \cdot (\Phi_d u_d) = \frac{-m_{dc}}{\rho_d}$$

Compute volume fraction

Inc., C. (2020). *COMSOL*. Retrieved from http://www.comsol.com/products/multiphysics/

Euler-Euler (EE) Model

Mass Balance

Continuity equation continuous phase mass balance and dispersed phase mass balance

$$\nabla \cdot (\Phi_c u_c) + \nabla \cdot (\Phi_d u_d) = \frac{m_{dc}}{\rho_c} - \frac{m_{dc}}{\rho_d} \qquad \Phi_c = 1 - \Phi_d$$

$$\nabla \cdot [(1 - \Phi_d) u_c + (\Phi_d u_d)] = m_{dc} \left(\frac{1}{\rho_c} - \frac{1}{\rho_d} \right)$$

Compute mixture pressure

Inc., C. (2020). *COMSOL*. Retrieved from http://www.comsol.com/products/multiphysics/

Euler-Euler (EE) Model

Momentum Balance

For fluid-solids mixtures where $\rho_d \gg \rho_c$, momentum balanced dispersed phase is modified in the manner of Enwald

Continuous phase (liposomes)

$$\rho_c \Phi_c \left[\frac{\partial}{\partial t}(u_c) + u_c \nabla \cdot (u_c)\right] = -\Phi_c \nabla p + \underbrace{\Phi_d \nabla \cdot \boldsymbol{\tau_d}}_{\nabla \boldsymbol{p_s}} + \Phi_c p_c \mathbf{g} + \mathbf{F}_{m,c} + \Phi_c \mathbf{F}_c - m_{dc}(u_{int} - u_c)$$

Dispersed phase (CS-MNPs)

$$\rho_d \Phi_d \left[\frac{\partial}{\partial t}(u_d) + u_d \nabla \cdot (u_d)\right] = -\Phi_d \nabla p + \underbrace{\Phi_d \nabla \cdot \boldsymbol{\tau_d}}_{\nabla \boldsymbol{p_s}} + \Phi_d p_d \mathbf{g} + \mathbf{F}_{m,d} + \Phi_d \mathbf{F}_d - m_{dc}(u_{int} - u_d)$$

Where

- $p_s = solid\ pressure (Pa)$
- $\tau = viscous\ stress\ tensor\ (Pa)$

Momentum balance was assumed Newtonian fluid

Inc., C. (2020). *COMSOL*. Retrieved from http://www.comsol.com/products/multiphysics/

Euler-Euler (EE) Model

Viscous Stress Tensors

Continuous phase (liposomes)

$$\tau_c = \mu_c^m \left(\nabla u_c + (u_c)^T - \frac{2}{3} (\nabla \cdot u_c) I \right)$$

Dispersed phase (CS-MNPs)

$$\tau_d = \mu_d^m \left(\nabla u_d + (u_d)^T - \frac{2}{3} (\nabla \cdot u_d) I \right)$$

Where $\mu_c^m, \mu_d^m = dinamyc\ viscosity\ (Pa)$

Inc., C. (2020). *COMSOL*. Retrieved from http://www.comsol.com/products/multiphysics/

Euler-Euler (EE) Model

Momentum Balance

Using nonconservative forms

Dispersed phase (CS-MNPs)

$$\rho_c \left[\frac{\partial}{\partial t}(u_d) + u_d \nabla \cdot (u_d)\right] = -\nabla p + \nabla \cdot \tau_d + \rho_d \mathbf{g} + \frac{\mathbf{F}_{m,d}}{d} + \mathbf{F}_d - \frac{m_{dc}(u_{int} - u_d)}{d}$$

Where

- $p = mixture\ pressure\ (Pa)$ equal for two phases
- $\tau = viscous\ stress\ tensor\ (Pa)$
- $\boldsymbol{g} = vector\ of\ gravitational\ acceleration\ (m/s^2)$
- $\mathbf{F}_m = interphase\ momentum\ transfer\ term\left({}^{N}/_{m^3}\right)$
- $\mathbf{F} = volume\ force\ term\left({}^{N}/_{m^3}\right)$
- $u_{int} = interphase\ velocity\ (m/s)$

Inc., C. (2020). *COMSOL*. Retrieved from http://www.comsol.com/products/multiphysics/

Euler-Euler (EE) Model

Viscosity Models

Dispersed phase (CS-MNPs)

Krieger Type

$$\mu_{mix} = \mu_c \left(1 - \frac{\Phi_d}{\Phi_{d,max}}\right)^{-2.5\Phi_{d,max}}$$

Where

Maximum packing limit $\Phi_{d,max} = 0.62$

Inc., C. (2020). *COMSOL*. Retrieved from http://www.comsol.com/products/multiphysics/

Euler-Euler (EE) Model

Damping functions - Wall BC

Lam and Bremhorst EE Model (LB)

$$E = 0$$

$$\varepsilon_w = v\left(\frac{\partial^2 k}{\partial y^2}\right)$$ Wall Function

Viscous stress tensor related term

Yang et al. EE Model (YS)

$$E = vv_t\left(\frac{\partial^2 U^2}{\partial y^2}\right)$$

$$\varepsilon_w = v\left(\frac{\partial^2 k}{\partial y^2}\right)$$ Wall Function

Viscous stress tensor related term

Inc., C. (2020). *COMSOL*. Retrieved from http://www.comsol.com/products/multiphysics/

Manufacturing Process

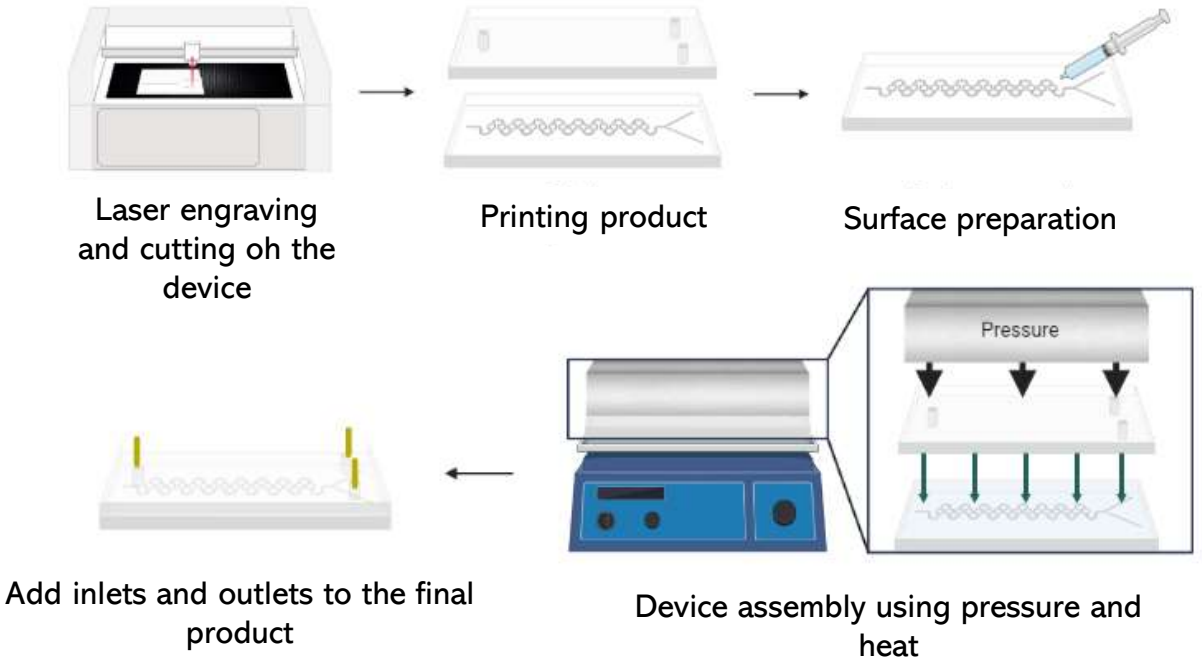

Figure 1. Manufacturing process

Geometries and Boundary conditions

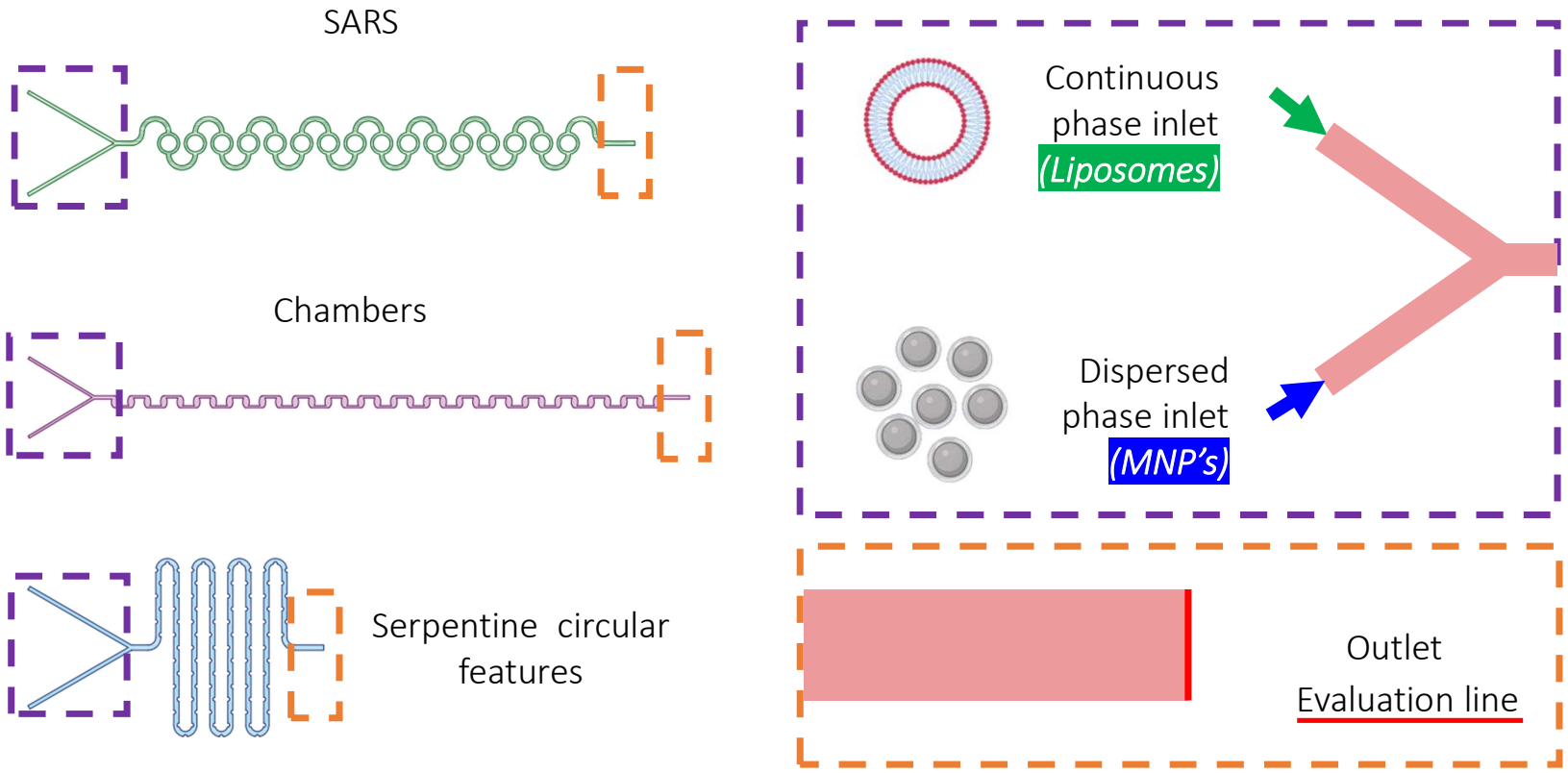

Figure 2. Geometries and boundary conditions, inlets, outlets and evaluation lines

Mesh selection

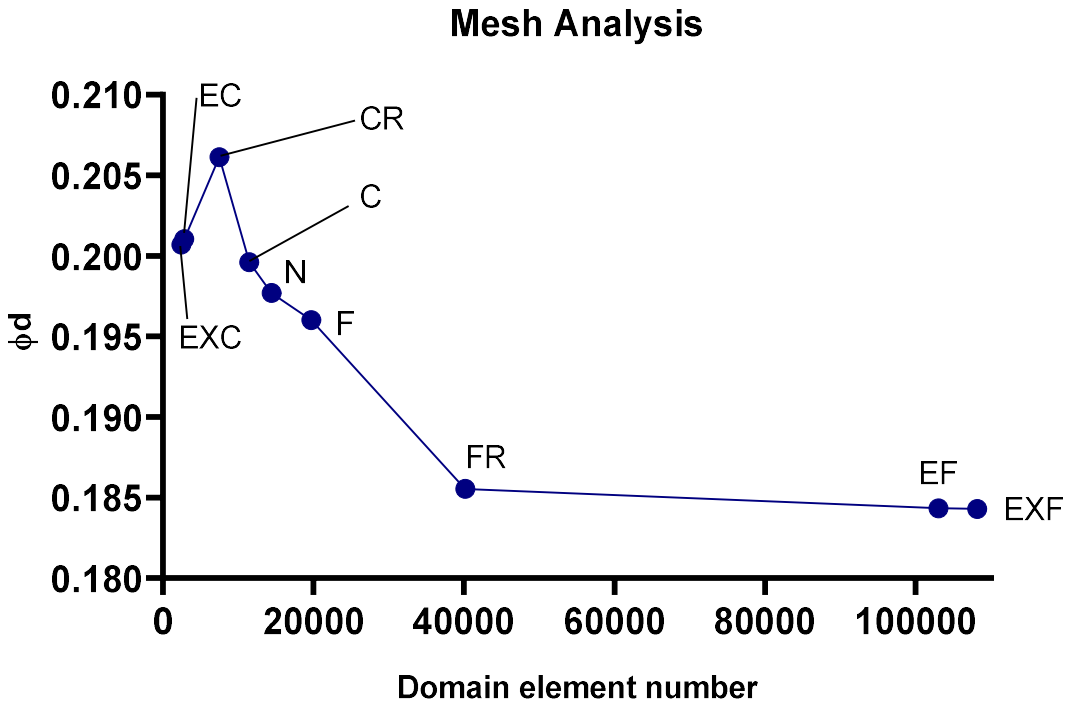

EXC: Extremely coarse
EC: Extra coarse
CR: Coarser
C:Coarse
N:Normal
F:Fine
FR: Finer
EF: Extra fine
EXF: Extremely fine

Figure 3. Mesh convergence analysis for SARS geometry. Complete mesh consist of 40175 domain elements

Inc., C. (2020). *COMSOL*. Retrieved from http://www.comsol.com/products/multiphysics/

Mesh selection

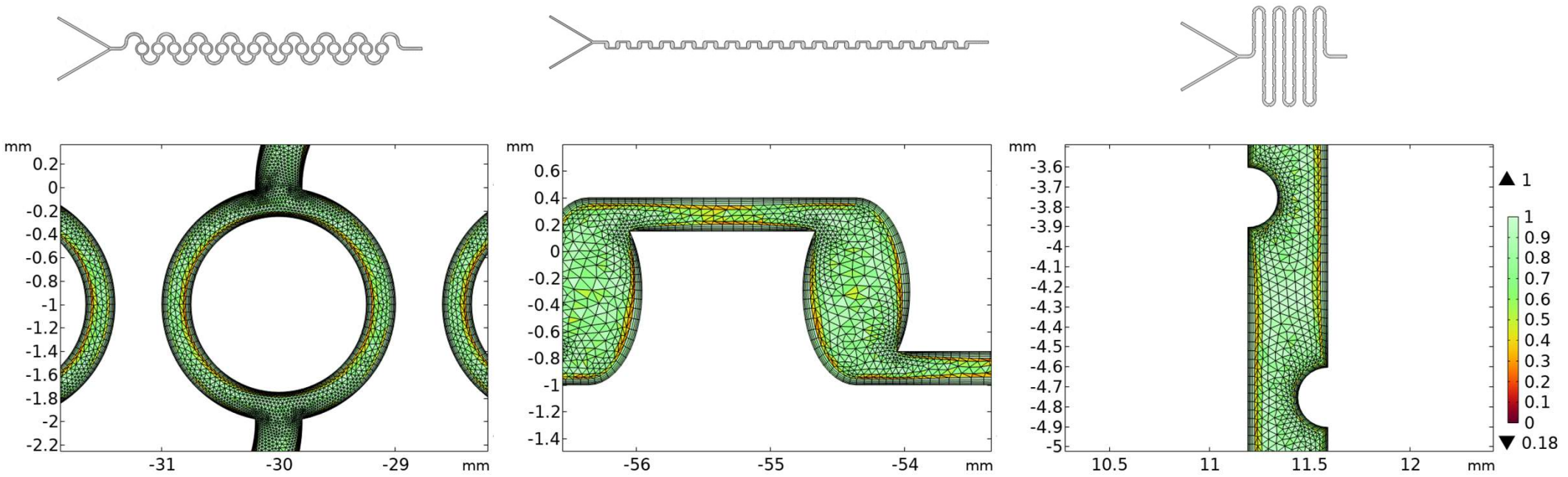

Figure 4. Mesh quality. Left to right: SARS, Chambers and Serpentine circular features geometry

Inc., C. (2020). *COMSOL*. Retrieved from http://www.comsol.com/products/multiphysics/

Dispersed phase Volume fraction

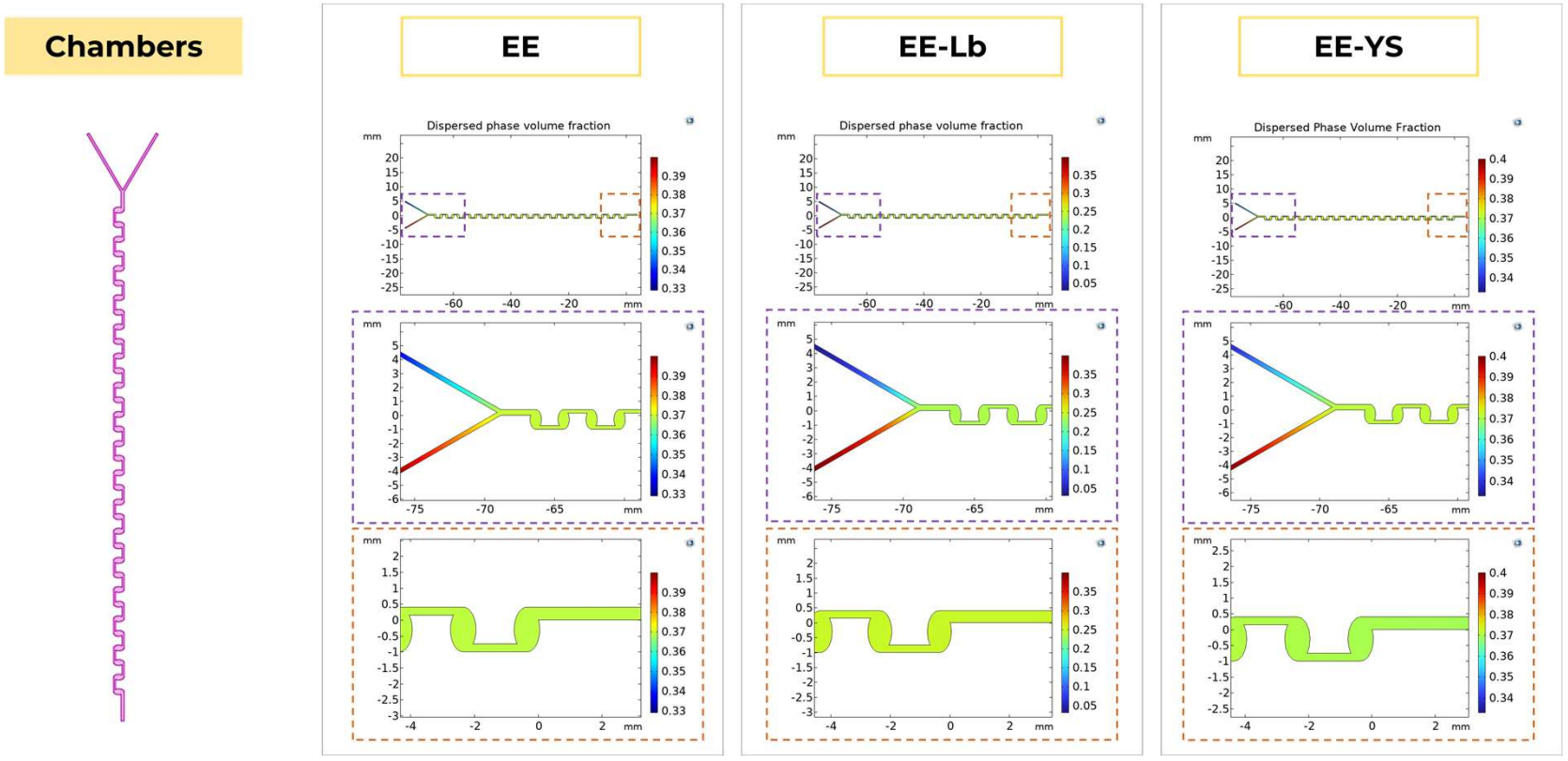

Figure 5. Dispersed phase volume fraction using variations in EE Model in chambers geometry

Inc., C. (2020). *COMSOL*. Retrieved from http://www.comsol.com/products/multiphysics/

Dispersed phase Volume fraction

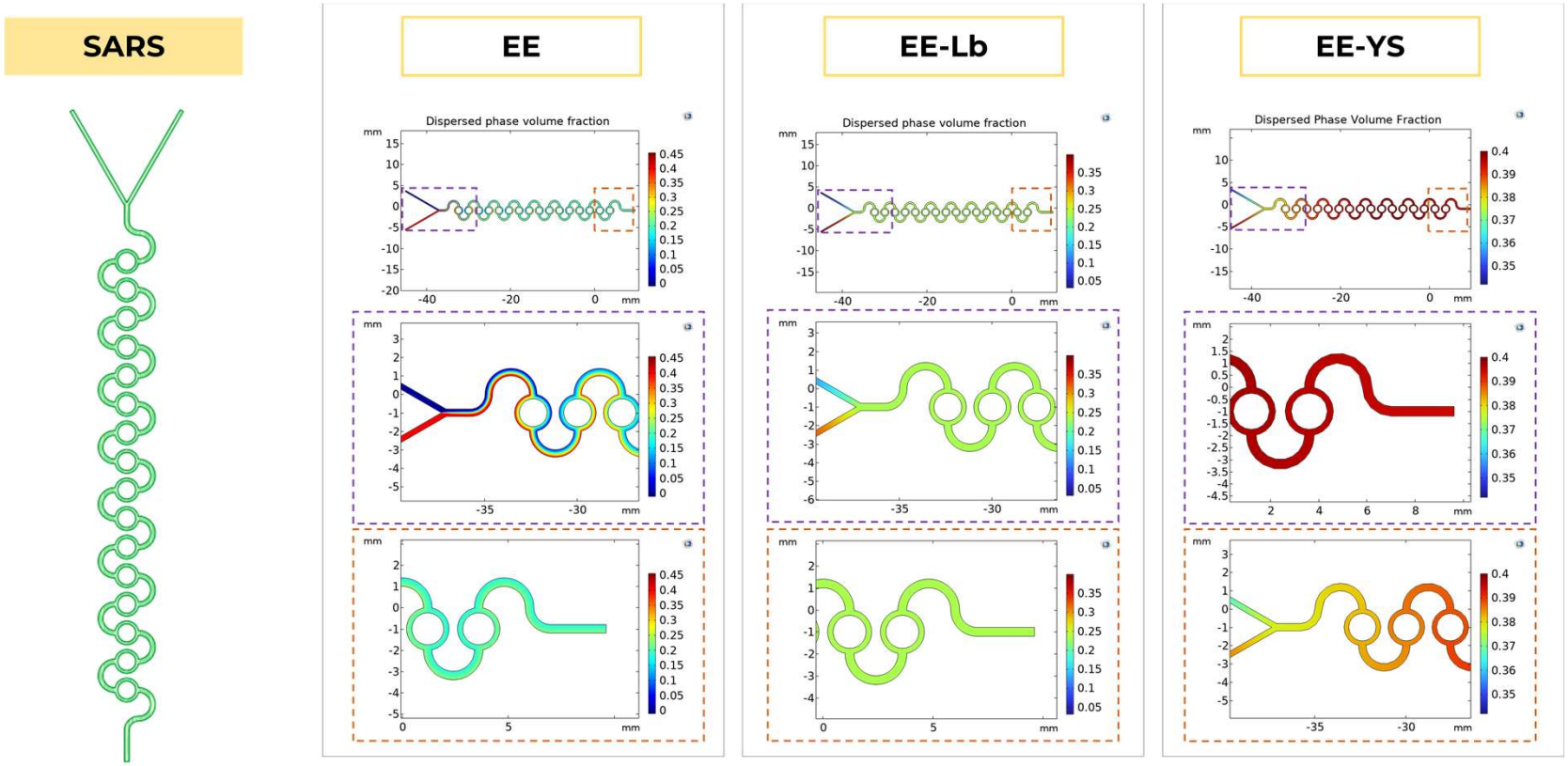

Figure 6. Dispersed phase volume fraction using variations in EE Model in SARS geometry

Inc., C. (2020). *COMSOL*. Retrieved from http://www.comsol.com/products/multiphysics/

Dispersed phase Volume fraction

Serpentine Circular Features

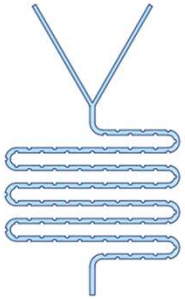

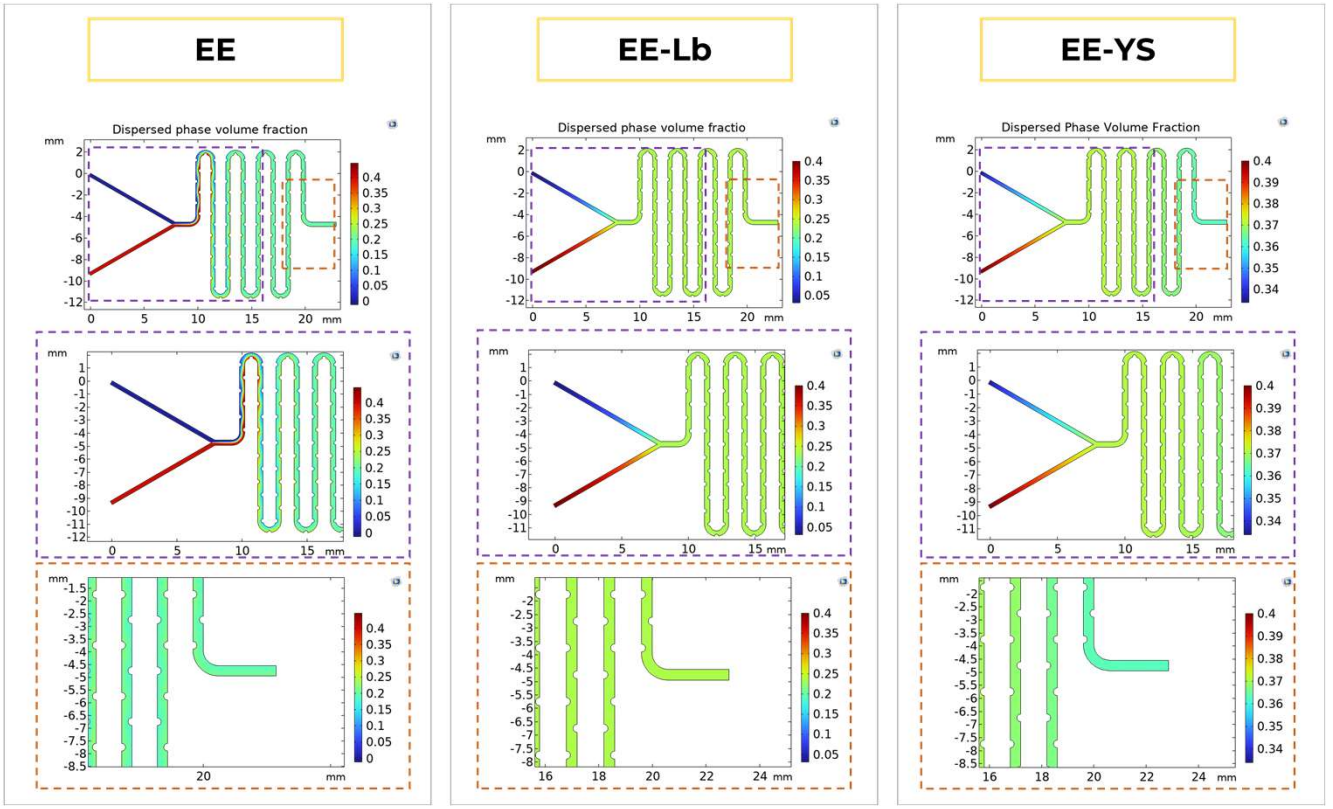

Figure 7. Dispersed phase volume fraction using variations in EE Model in serpentine CF geometry

Encapsulation Efficiency (EE%)

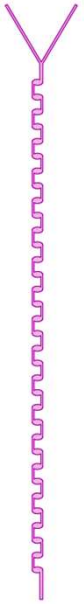

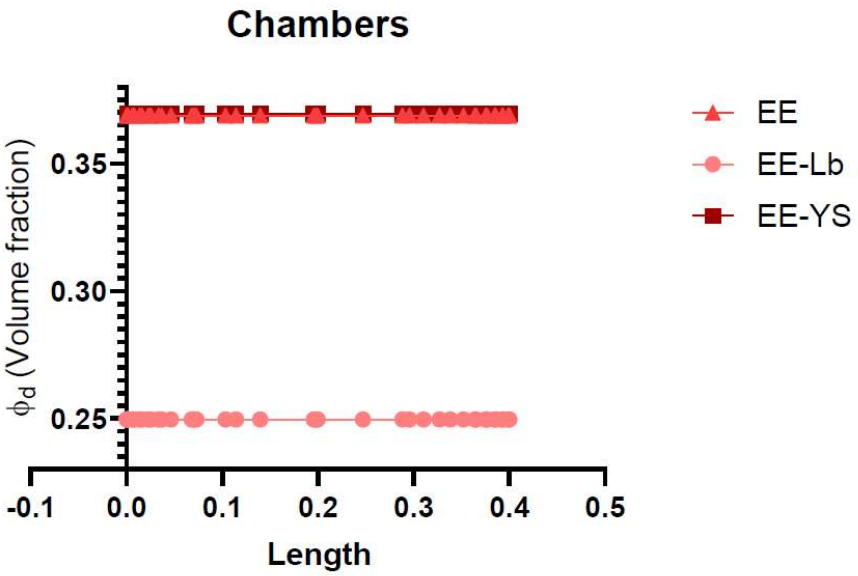

$$EE\% = \left(\frac{\phi_{d,min}}{\phi_d / FRR}\right) \times 100$$

$$EE\ EE\% = 38.69$$

$$EE\ Lb\ EE\% = 58.48$$

$$EE\ Ys\ EE\% = 98.69$$

Figure 8. Encapsulation efficiency Volume fraction variation by length in chambers geometry

Encapsulation Efficiency (EE%)

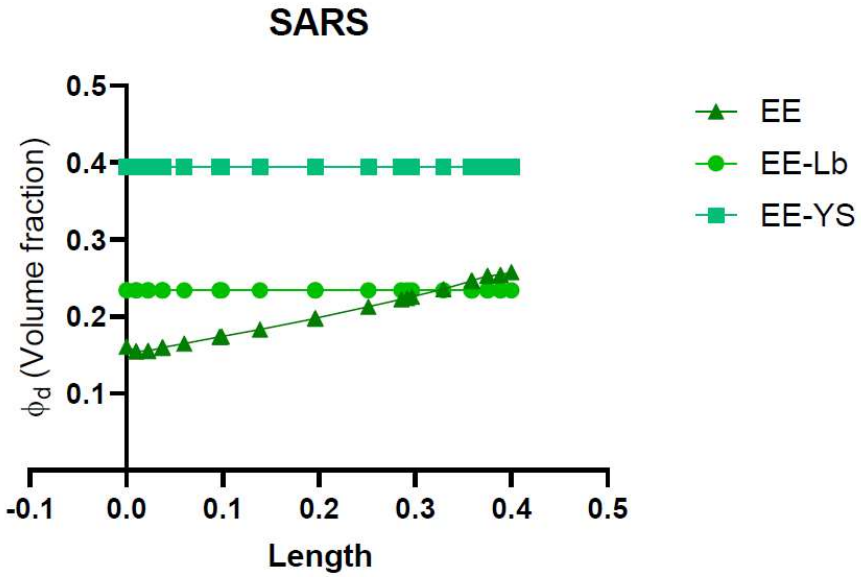

$$EE\% = \left(\frac{\phi_{d,min}}{\phi_d/_{FRR}}\right) \times 100$$

$$EE\ EE\% = 47.58$$

$$EE\ Lb\ EE\% = 58.71$$

$$EE\ Ys\ EE\% = 90.79$$

Figure 9. Encapsulation efficiency Volume fraction variation by length in SARS geometry

Encapsulation Efficiency (EE%)

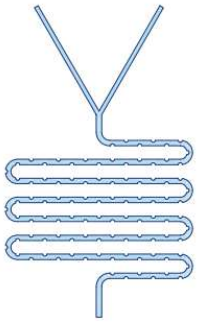

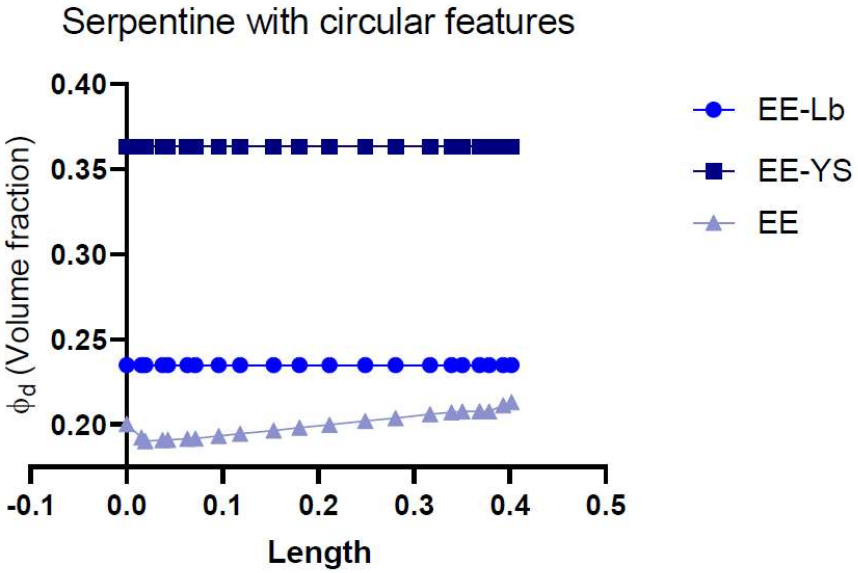

$$EE\% = \left(\frac{\phi_{d,min}}{\phi_d/_{FRR}}\right) \times 100$$

$$EE\ EE\% = 92.18$$

$$EE\ Lb\ EE\% = 62.38$$

$$EE\ Ys\ EE\% = 92.33$$

Figure 10. Encapsulation efficiency Volume fraction variation by length in serpentine CF geometry

Encapsulation Efficiency (EE%)

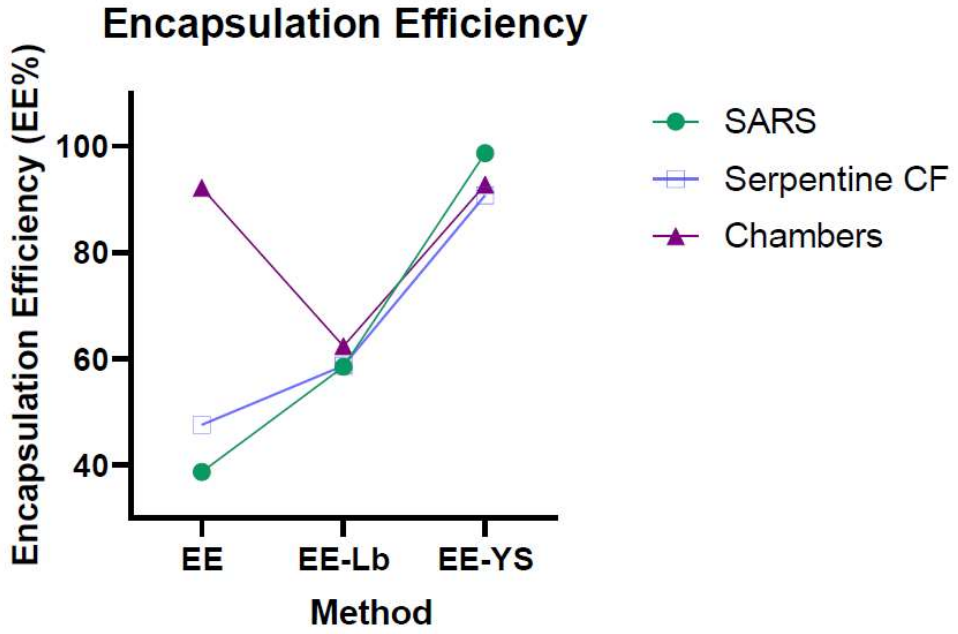

$$EE\% = \left(\frac{\phi_{d,min}}{\phi_d / FRR}\right) \times 100$$

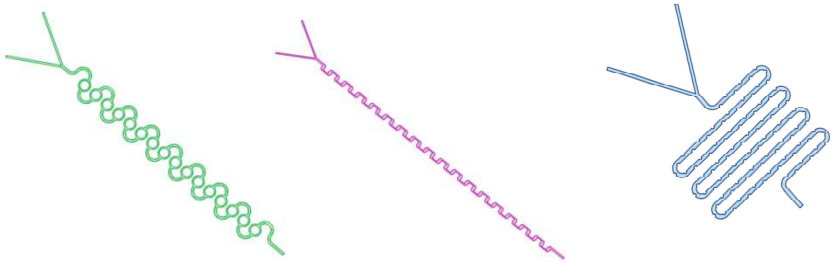

$$SARS > Chambers > Serpentine\ CF$$

Figure 11. Encapsulation efficiency Volume fraction variation by length. Comparative graph

Encapsulation Efficiency (EE%)

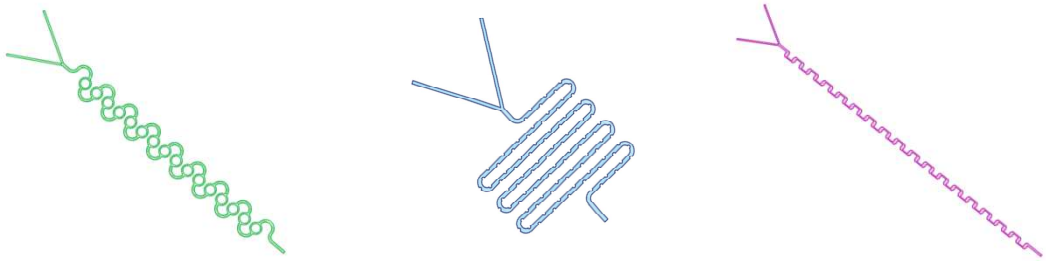

Table 2. Encapsulation efficiency contrast between geometries and math models

Model/Geometry	SARS	Serp CF	Chambers
EE	38.69	47.58	92.18
EE-Lb	58.48	58.71	62.38
EE-YS	98.69	90.79	92.33

Conclusions

- By implementing near-wall damping functions in the Euler-Euler approximation, it is possible to model the mixing process more effectively as they address the **turbulence phenomena at low Reynolds numbers by balancing the rate of of kinetic energy dissipation** and thus ensure a better encapsulation process.
- The LB and YS turbulence models had the best performance, obtaining EE% between **58.48-62.38% and 90.79-98.69%** respectively.
- The Euler-Euler model was sufficient for the analysis; however, **stochastic** processes related to the mixing process will be considered in future work.
- According to the YS model with damping functions, the micromixer with the channel SARS geometry led to the highest EE%, i.e., 98.69%.

Universidad de los Andes
Colombia

MDPI

IECBM 2022

Modeling and simulation of magnetoliposome formation by encapsulation of core-shell, magnetite-chitosan nanoparticles in liposomes enabled by a low-cost microfluidic system.

Andres D. Mantilla BSc.

Juan C. Cruz PhD

Carolina Muñoz-Camargo PhD

Thank you

for your attention

GINIB

Grupo de Investigación en Nanobiomateriales, Ingeniería Celular y Bioimpresión